Journal of the European Ceramic Society **15** (1995) 463–468

0955-2219/95/$9.50

0955-2219(95)00007-0

The Preparation, Characterization and Electrical Properties of Electroceramics made of Copper–Cobalt Manganite Spinel: $Mn_{2\cdot6-x}Co_{0\cdot4}Cu_xO_4$, $0 \leq x \leq 1$

R. Legros, R. Metz[a] & A. Rousset

Laboratoire de Chimie des Matériaux Inorganiques, U.R.A. - C.N.R.S. 1311, 118, route de Narbonne, 31062 Toulouse Cedex, France

(Received 30 November 1993; revised version received 19 July 1994; accepted 12 December 1994)

Abstract

In this paper we report our results on the preparation and characterization of copper–cobalt manganites, $Mn_{2\cdot6-x}Co_{0\cdot4}Cu_xO_4$ ($0 \leq x \leq 1$), obtained from coprecipitated oxalate precursors. Powder and single phase ceramics have been characterized by means of X-ray diffraction (XRD) and electrical conductivity measurements. The results of both characterization techniques are indicative of the ionic distribution for the copper–cobalt manganites solid solution studied: $Mn^{2+}_{0.6-x}Co^{2+}_{0.4}Cu^{+}_{x}\,[Mn^{3+}_{2-x}\,Mn^{4+}_{x}]\,O^{2-}_{4}$; with $0 \leq x \leq 0{\cdot}6$, $Co^{2+}_{0.4}\,Cu^{+}_{0.6}\,[Cu^{2+}_{y}Mn^{3+}_{1.4-2y}\,Mn^{4+}_{0.6+y}]\,O^{2-}_{4}$; with $0{\cdot}6 < x \leq 1$ and $y = x - 0{\cdot}6$.

1 Introduction

Thermistors with Negative Temperature Coefficient of Resistance (NTC) are semiconducting thermally sensitive resistors whose primary function is to exhibit a wide change in electrical resistance with a change in body temperature. These electroceramics are often constituted of spinel structure transition metal manganites with formula: $Mn_{3-x'-x}\,Ni_{x'}\,M_x\,O_4$ ($0 \leq x+x' \leq 1{\cdot}5$; M = Ni, Co, Cu...).

The purpose of this paper is to present the study of manganites without nickel which is often present in industrial NTC thermistors.

The transition metal oxides have aroused considerable interest regarding the valency and the cationic distribution among tetrahedral and octahedral sites in the spinel structure. Many workers using different experimental techniques have sought to resolve this problem. However, the cationic distribution of manganites depends on the preparation conditions. For instance, Kulkarni *et al.*[1] have established from X-ray absorption spectroscopy that the defined compound $CoCuMnO_4$ presents a tetragonal structure with the cationic distribution: $Co^{2+}[Mn^{4+}Cu^{2+}]\,O^{2-}_4$. (the square brackets indicate octahedral sites). However, using a different route Brabers *et al.*[2] prepared a single-phase cubic spinel with the following distribution: $Cu^{+}_{0.65}Mn^{3+}_{0.35}[Cu^{2+}_{0.35}Co^{3+}_{1}Mn^{4+}_{0.65}]O^{2-}_4$. They called into question Kulkarni's preparation.

Hence, to avoid any substantial deviation from an intended composition, it seems necessary to study solid solution rather than defined compounds since one may reasonably assume that the oxidation states and the distribution of cations vary continually with the composition.

Kshirsagar *et al.*[3] studied the solid solution, $Co_xCu_{1-x}[Mn_2]O_4$, and showed that for $x < 0{\cdot}5$ the structure becomes cubic. In this solid solution the manganese is fixed which differs from the present paper in which we have studied the substitution of copper for manganese in the cobalt manganite with formula: $Mn_{2\cdot6}Co_{0\cdot4}O_4$.

Cobalt manganites $Mn_{3-x}Co_xO_4$ for $0 \leq x \leq 1$ have been previously studied.[4–7] These components have tetragonal structure and their cation distribution can be deduced from that of hausmannite as given by $Mn^{2+}\,[Mn^{3+}_2]\,O^{2-}_4$ by substituting essentially Mn with Co on tetrahedral sites implying a structural formula of type $Mn^{2+}_{1-x}Co^{2+}_x\,[Mn^{3+}_2]\,O^{2-}_4$. This structural description accounts for their tetragonal structure characterized by their stability up to very high temperatures and their practical insulating properties.

By analogy with copper manganites, we have tried to create Mn^{3+}–Mn^{4+} couples in octahedral sites which resulted in a dramatic decrease in the electrical resistivity.[8–9]

[a] Present address: Pharmacie Centrale de France, Quai Jean Jaurès - BP 57, 07800 La Voulte-Sur-Rhône, France.

Table 1. Quenched temperatures and lattice parameters of single-phase oxide powders: $Mn_{2\cdot6-x}Co_{0\cdot40}Cu_xO_4$

x	*Quenched*	*Lattice parameters (nm)*			
	temperature °C	*a*	*c*	$a' = 3\sqrt{a^2c}$	*c/a*
·00	1100	·812	·944	·854	1·16
·05	1000	·813	·930	·850	1·14
·10	1050	·813	·932	·851	1·15
·20	1050	·813	·924	·849	1·14
·30	900	·814	·911	·845	1·12
·39	900	·816	·902	·844	1·10
·50	900	·817	·891	·841	1·09
·59	900	·820	·882	·840	1·08
·66	900	·821	·873	·838	1·06
·69	900	·821	·871	·837	1·06
·79	900	·835	·835	·835	1
·90	900	·835	·835	·835	1
1·0	900	·834	·834	·834	1

2 Experimental Procedure

2.1 Sample preparation of powders

The powders were obtained from the decomposition of oxalic precursors prepared by coprecipitation in aqueous solution from $MnCl_2$, $6H_2O$, $CoCl_2$, $6H_20$ and $CuCl_2$, $6H_2O$ and ammonium oxalate $(NH_4)_2C_2O_4$, H_2O at 25°C.

Simple thermal decompositions in air of the precipitated oxalic precursors leads to a mixture of oxides. Therefore, by analogy with the preparation of copper manganite spinels,[9] a long stage at high temperature (to increase the diffusion of the oxides), followed by a quench treatment in water (to stabilize the high temperature structure at room temperature) has been used. These heat treatments in air, with different profiles depending upon the compositions of powders prepared yield metastable single-phase oxides and are depicted in Table 1.

2.2 Sample preparation of ceramics

The earlier preparation of powder with a single-phased spinel structure was of great use in preparing ceramics with a single-phased spinel structure. To obtain well densified ceramics, the previous oxide powders were first pressed into disc form (6 mm diameter and 2 mm thickness) under 7 kbar. Then, the green discs were fired for 4 h at a temperature depending upon the amount of copper. After the sintering the samples were cooled at a rate of 120°C per hour, to the temperature used to obtain single-phased powders and were kept at this temperature for 24 h. The final cooling was a quench in water to stabilize the high temperature structure at room temperature.

It is worth noticing that the single-phased powders were difficult to sinter. Table 2 shows the evolution of densification depending on various sintering temperatures for the given composition: $Mn_{2\cdot20}Co_{0\cdot4}Cu_{0\cdot39}O_4$. It appears that for each composition, there is an optimal sintering temperature (Table 3). Moreover, for certain compositions ($x > 0\cdot5$), we report the phenomenon of exaggerated growth of manganite grains which led to grain sizes up to 500 μm. Eventually, the ceramics cracked or became extremely brittle.

Table 2. Sintering temperatures and densification for the given single-phase ceramic: $Mn_{2\cdot20}Co_{0\cdot41}Cu_{0\cdot39}O_4$

Sintering temperature (°C)	*Densification (%)*
1100	94·5
1130	98
1150	95
1170	94
1200	93

2.3 X-ray diffraction

XRD powder patterns were recorded at room temperature using an automatic diffractometer (Siemens D 501, CoKα radiation). The standard error on parameters was less than ± 0·0005 nm.

2.4 Measurement of electrical properties of ceramics

Samples for electrical measurements were prepared by depositing silver electrodes on the opposite faces of the discs formed and were subjected to thermal treatment at 850°C, so as to make good ohmic contact with the ceramics.

The d.c. resistivity was deduced by classical resistance measurements made at 25 ± 0·05°C and using the relationship $\rho = RS/l$, with R, the electrical resistance in Ohms (Ω); S the area of the specimen in cm^2 and l the thickness of the specimen in cm. Another d.c. resistance measurement was carried out at 85 ± 0·05°C so as to deduce the band gap-related constant B from the classical law of semiconductors $\rho = \rho_0\exp(B/T)$ with $B = \Delta E/2k$.

Table 3. Sintering temperatures used to obtain well densified single-phase ceramics: $Mn_{2\cdot6-x}Co_{0\cdot4}Cu_xO_4$

x	*Theoretical density*	*Densification* (%)	*Sintering temperature* (°C)
·00	4·92	93	1130
·05	4·95	93	1130
·20	5·05	95	1130
·30	5·13	95·5	1130
·39	5·20	98	1130
·50	5·25	95	1130
·59	5·36	97·5	1110
·66	5·40	94·5	1080
·79	5·42	97	1050
·90	5·42	94	1030
1·00	5·44	95·5	1020

3 Results and Discussion

3.1 XRD analyses

3.1.1 Cation distribution of manganite powders

The variation of the lattice parameters of single-phased powders as a function of the copper content is reported in Table 1. Most of the solid solutions $Mn_{2\cdot6-x}Co_{0\cdot4}Cu_xO_4$ were found to be tetragonally distorted from cubic symmetry. The tetragonal distortion $c/a > 1$ decreased with copper content and disappeared for $x \geq 0\cdot79$.

The substitution of copper in the matrix $Mn^{2+}_{0.6}Co^{2+}_{0\cdot4}[Mn^{3+}_2]\ O^{2-}_4$ could be interpreted by one of the four theoretical limiting ionic configurations as follows:

(a) $Mn^{2+}_{0.6-x}Co^{2+}_{0\cdot4}\ Cu^{+}_x\ [Mn^{3+}_{2-x}\ Mn^{4+}_x]\ O^{2-}_4$;
with $0 \leq x \leq 0\cdot6$;

(b) $Mn^{2+}_{0.6-x}Co^{2+}_{0\cdot4}\ Cu^{2+}_x\ [Mn^{3+}_2]\ O^{2-}_4$;
with $0 \leq x \leq 0\cdot6$;

(c) $Mn^{2+}_{0.6}Co^{2+}_{0\cdot4}\ [Cu^{+}_xMn^{3+}_{2-3x}Mn^{4+}_{2x}]\ O^{2-}_4$;
with $0 \leq x \leq 0\cdot66$;

(d) $Mn^{2+}_{0.6}Co^{2+}_{0\cdot4}\ [Cu^{2+}_x\ Mn^{3+}_{2\ 2x}Mn^{4+}_x]\ O^{2-}_4$;
with $0 \leq x \leq 1$.

However, according to the work of Baffier and Huber,[10] the tetragonal distortion in the ferromanganite spinel structure is created by the presence of cations Mn^{3+} on the octahedral sites. Moreover, they have shown that a minimum concentration of Mn^{3+} cations in octahedral sites is necessary to raise a cooperative Jahn–Teller effect. This minimum concentration is about 50%. Thus there is a correlation between the concentration of cations Mn^{3+} in octahedral sites and the macroscopic distortion observed by X-ray diffraction.

The formulae (a), (c) and (d) might explain the decrease of tetragonal distortion as a function of copper content by diminishing the Mn^{3+} ion content in B sites, e.g. by decreasing the Jahn–Teller effect of the cations Mn^{3+} ($t^3_{2g}\ e^1_g$) localized in octahedral sites. However the components (c) and (d) cannot fit with the experimental tetragonal distortion observed for $0 \leq x < 0\cdot79$, because for $x \geq 0\cdot33$ and $x \geq 0\cdot5$ respectively, the distortion of the spinel structure should disappear while the concentration of Mn^{3+} in octahedral sites drops below the 50% critical value necessary to raise a cooperative Jahn–Teller effect. In the case of formula (b), the increased amount of copper (II) in tetrahedral sites must be responsible for a Jahn–Teller effect $c/a < 1$ and thus for the overall decrease of the distortion.

The cubic spinel structure is preserved when different kinds of cation occupy a spinel site. From this Poix[11] defined two parameters: $dCA = \Sigma i\ xi\ (CA_i - 0)$ and $dCB = \Sigma i\ xi/(CBi - 0)/2$ where dCA and dCB are the mean values of the 'oxygen–cation' distance in tetrahedral and octahedral sites respectly. The lattice parameter a of the cubic structure spinel is related to the dCA and dCB according to

$$a = 2\cdot0995\ dCA + (5\cdot8182\ dCB^2 - 1\cdot4107\ dCA^2)^{1/2}$$

Table 4. Anion–cation distance in tetrahedral and octahedral sites of cubic spinel structure[11]

Cations	*Cation–oxygen (nm)*	
	A sites	*B sites*
Mn^{2+}	·2041	·2220
Mn^{3+}	—	·2045
Mn^{4+}	—	·1843
Co^{2+}	·1967	—
Cu^{+}	·2070	·2281
Cu^{2+}	·1940	·2150

It may be seen that the theoretical lattice parameters could be calculated for various cation distributions among the two sublattices. When the phases crystallise in a tetragonally deformed spinel structure it is possible to replace a (cubic parameter) by $a' = \sqrt[3]{a^2c}$ (cubic/root of volume cell). Thus, it is possible, knowing the characteristic bond distances manganese–oxygen, cobalt–oxygen and copper–oxygen (Table 4) to calculate from the cation distributions (a), (b), (c) and (d), the theoretical decrease of the cubic parameter a (or a') as a function of the amount of copper substituted in the manganite: $Mn_{2\cdot6-x}Co_{0\cdot4}Cu_xO_4$.

The variation of the lattice parameter, a', of $Mn_{2\cdot6-x}Co_{0\cdot4}Cu_xO_4$ powders as a function of the copper content, x, calculated for the cation distributions (a), (b), (c) and (d), is compared with the experimental data (Fig. 1). It appears very clear that the hypothetical distributions (b) and (d) cannot fit with the experimental results. It is difficult to choose between the formulae (a) and (c); however the previous discussion about the cooperative Jahn–Teller effect shows that the distribution (c) involves a tetragonal–cubic transition for $x > 0\cdot33$ instead of an experimental transition observed for $x > 0\cdot66$. Thus, the most probable distribution among the four extreme hypothetical substitution processes is:

(a) $Mn^{2+}_{0.6-x}Co^{2+}_{0\cdot4}Cu^{+}_x\ [Mn^{3+}_{2-x}\ Mn^{4+}_x]\ O^{2-}_4$;
with $0 \leq x \leq 0\cdot6$.

According to this last cation distribution with $0 \leq x \leq 0\cdot6$, for $x > 0\cdot6$, the copper should substitute the manganese located in octahedral sites. Two different theoretical substitutions could appear;

(e) $Co^{2+}_{0\cdot4}Cu^{+}_{0\cdot6}\ [Cu^{+}_yMn^{3+}_{1.4-3y}Mn^{4+}_{0\cdot6+2y}]\ O^{2-}_4$;

(f) $Co^{2+}_{0\cdot4}Cu^{+}_{0\cdot6}\ [Cu^{2+}_yMn^{3+}_{1.4-2y}Mn^{4+}_{0\cdot6+y}]\ O^{2-}_4$;
with $y = x\text{-}0\cdot6$ and $0 < y < 0\cdot4$

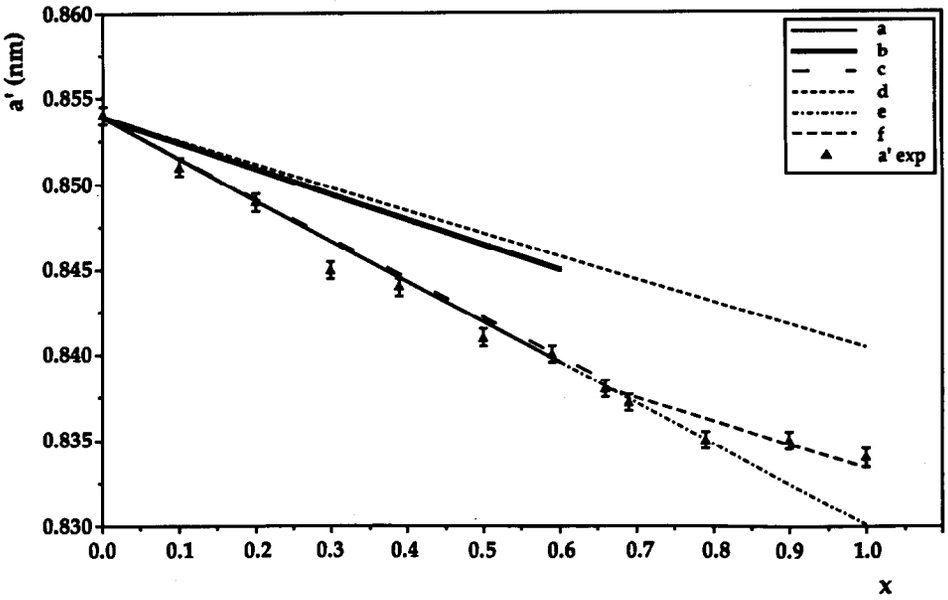

Fig. 1. Theoretical changes of the lattice parameter a' and equations to straight lines calculated for the following cationic distributions:

(a) $Mn^{2+}_{0.6-x}Co^{2+}_{0.4}Cu^{+}_{x}\,[Mn^{3+}_{2-x}Mn^{4+}_{x}]\,O^{2-}_{4}$ → a' = –0·239x + 8·539;

(b) $Mn^{2+}_{0.6-x}Co^{2+}_{0.4}Cu^{2+}_{x}\,[Mn^{3+}_{2}]\,O^{2-}_{4}$ → a' = –0·147x + 8·539;

(c) $Mn^{2+}_{0.6}Co^{2+}_{0.4}[Cu^{+}_{x}Mn^{3+}_{2-2x}Mn^{4+}_{x}]\,O^{2-}_{4}$ → a' = –0·233x + 8·539;

(d) $Mn^{2+}_{0.6-x}Co^{2+}_{0.4}[Cu^{2+}_{x}Mn^{3+}_{2-x}Mn^{4+}_{x}]\,O^{2-}_{4}$ → a' = –0·134x + 8·539;

(e) $Co^{2+}_{0.4}Cu^{+}_{04}[Cu^{+}_{y}Mn^{3+}_{1.4-3y}Mn^{4+}_{0.6+2y}]\,O^{2-}_{4}$ → a' = –0·235y + 8·536;

(f) $Co^{2+}_{0.4}Cu^{+}_{06}[Cu^{2+}_{y}Mn^{3+}_{1.4-2y}Mn^{4+}_{0.6+y}]\,O^{2-}_{4}$ → a' = –0·135y + 8·476.

– Experimental lattice parameters ī as a function of copper content x and equations to straight lines calculated for: $0 < x < 0{\cdot}6$ a' = – 0·238x + 8·534 close to equations (a) and (c); $0 < y < 0{\cdot}4$ a' = – 0·086 + 8·476 close to equation (f).

In contradiction to the formula (e) the experimental data fits well to the (f) line corresponding to the substitution of copper II to manganese in octahedral sites (Fig. 1). Thus, for $x > 0{\cdot}6$ the closer hypothetical cation distribution in these spinels is:

(f) $Co^{2+}_{0.4}Cu^{+}_{0.6}\,[Cu^{2+}_{y}Mn^{3+}_{1.4-2y}Mn^{4+}_{0.6+y}]\,O^{2-}_{4}$

3.1.2 Cation distribution of manganite ceramics

The diffraction analysis revealed the presence of pure spinel structure. The results concerning the lattice parameter values (Table 5), are very close to those observed with spinel powders (Table 1). Hence, we assume that the ionic distribution of the powder samples doesn't differ from the ceramics.

Table 5. Structure and lattice parameters of single-phase ceramics: $Mn_{2.6-x}Co_{0.4}Cu_xO_4$ (to be compared with Table 1)

x	*Spinel structure*	*Lattice parameter (nm)*		
		a	c	a'
·00	tetragonal	·812	·944	·854
·05	tetragonal	·812	·932	·850
·20	tetragonal	·815	·917	·848
·30	tetragonal	·814	·916	·847
·39	tetragonal	·816	·904	·844
·50	tetragonal	·817	·895	·842
·59	tetragonal	·819	·882	·839
·66	tetragonal	·820	·880	·840
·79	cubic	·835	—	—
·90	cubic	·834	—	—
1·00	cubic	·834	—	—

3.2 Electrical properties of ceramics

The experimental data are reported in Table 6. The electrical resistivity of copper–cobalt manganite ceramics decreases with copper ion content until a minimum of resistivity for $x = 0{\cdot}79$ (Fig. 2).

The substitution of copper ions for manganese ions in insulating spinel material, $Mn_{2.6}Co_{0.4}O_4$, gives rise to a semiconductor. The resistivity of the thermistors can reach several Ω cm. The con-

Table 6. Electrical data of monophased ceramics: $Mn_{2.6-x}Co_{0.4}Cu_xO_4$

x	*Spinel structure*	*Densification (%)*	*ρ (Ω·cm)*	*B (K)*
·00	tetragonal	93	$> 2{\cdot}10^6$	—
·05	tetragonal	93	880 000	5360
·20	tetragonal	95	1000	3100
·30	tetragonal	95·5	570	3080
·39	tetragonal	98	310	2970
·50	tetragonal	95	170	2900
·59	tetragonal	97·5	70	2850
·66	tetragonal	94·5	27	2750
·79	cubic	97	7	2490
·90	cubic	94	14	2600
1·00	cubic	95·5	40	2590

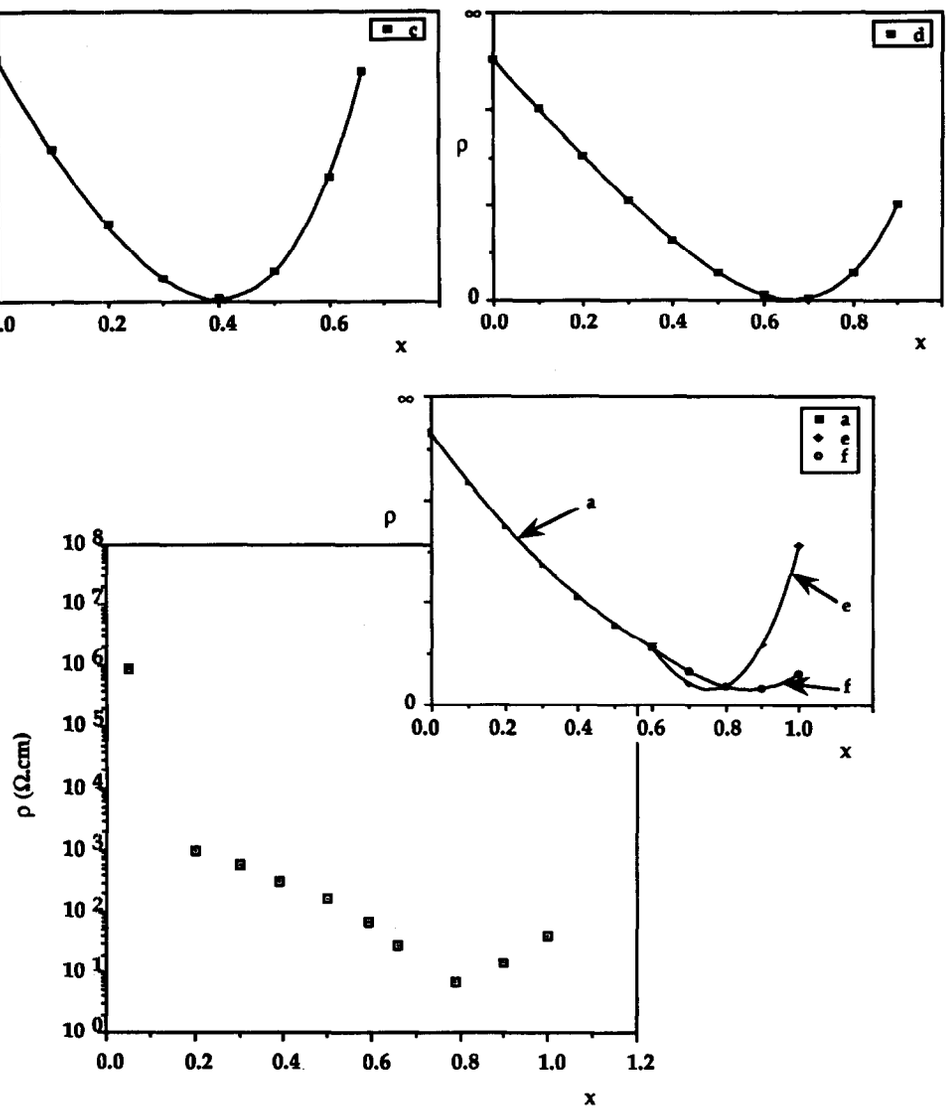

Fig. 2. ⊡ Experimental change of resistivity as a function of the copper content x. Theoretical variation of the resistivity according to the cationic distributions: (a) with $0 < x < 0{\cdot}6$ plus (e) and (f) with $0 < y < 0{\cdot}4$; distributions (c) and (d) with Cu II in octahedral sites.

ductivity of these components is dependent on the presence in the octahedral sites of Mn^{3+} and Mn^{4+}.

The electrical conductivity of a small polaron conductor can be written as[12]

$$\sigma = \frac{\sigma'_o}{T} NC(1-C) \exp\left(\frac{-E_H}{KT}\right) \text{with } \sigma'_o = \frac{N_{oct} e^2 d^2 \nu_o}{K}$$

where N_{oct} is a concentration per cm^3 of octahedral sites, d is a jump distance for the charge carrier, ν_o is the lattice vibrational frequency associated with conduction, K is Boltzmann's constant, e the electronic charge, N is a concentration per formule unit of sites which are available to the charge carriers, C is a fraction of available sites which are occupied by the charge carriers and E_H is a hopping energy.

The term NC (1-C) can be rewritten as

$$NC(1-C) = \frac{(Mn^{3+}_{oct})\,(Mn^{4+}_{oct})}{(Mn^{3+}_{oct}) + (Mn^{4+}_{oct})}$$

which represent the probability of finding Mn^{3+} - Mn^{4+} pairs in octahedral sites.

At first approximation, we take into account only the variation of the last ratio. Thus, the theoretical variation of resistivity can be plotted against copper content and compared to the experimental curve: $\rho = f(x)$. An inspection of the theoretical variations of resistivity with x calculated for the four hypothetical configurations shows an insulating character for formulae (b) (only Mn^{3+} in octahedral site) and a minimum of resistivity ($\partial(C(1-C)/\partial x=0$) with formulae (c) x = 0·4 (Fig. 2 curve *c*) and formulae (d) for x = 0·66 (Fig. 2 curve *d*). The experimental shape of the variation of resistivity (Fig. 2) with copper content does not present a minimum for x = 0·4 or x = 0·66. However, for $0{\cdot}2 \leq x \leq 0{\cdot}4$ the curve presents a slope change and hence, it should be possible that a small amount of copper be present in octahedral sites.

However, the theoretical variation of the resistivity, shown in curve *a* and *f* of Fig. 2, calculated from hypothetical configurations (a) and (f) selected from the earlier XRD study, fits the best

with the experimental data. For $0 \leq x \leq 0{\cdot}6$, the theoretical resistivity is proportional to $(2\text{-}x)x/4$ and the resistivity is expected to decrease continuously for $0 \leq x \leq 0{\cdot}6$. The minimum of resistivity should be for 0·87 ($\partial(C(1\text{-}C)/\partial y=0$) and not for 0·8 (experimental data). This slight misfit could be due to the fact that we have only taken into account the variation of density of charge carriers to calculate the theoretical variation of the resistivity; for instance the variation of the lattice volume (and hence, the hopping distance) which decreases for $0 \leq x \leq 1$ was not considered.

4 Conclusion

Precipitated oxalic have been employed to prepare oxides and ceramics with single-phased spinel structure: $Mn_{2\cdot6-x}Co_{0\cdot4}Cu_xO_4$, $0 \leq x \leq 1$. Powder XRD analysis both from powder and ceramic single-phase sample revealed the presence of a single phase having a tetragonally distorted spinel structure; the tetragonal distortion, $c/a > 1$, decreased with copper content and disappeared for $x \geq 0{\cdot}79$. The XRD powder study and the comparison of experimental curves with the calculated ones for electric resistivity measurements implemented on ceramics indicated that the cation distribution in these spinels is close, both at the powder and ceramic states, to:

$$Mn^{2+}_{0.6-x}Co^{2+}_{0\cdot4}\ Cu^{+}_{x}\ [Mn^{3+}_{2-x}\ Mn^{4+}_{x}]\ O^{2-}_{4};$$
with $0 \leq x \leq 0{\cdot}6$,

$$Co^{2+}_{0\cdot4}Cu^{+}_{0\cdot6}\ [Cu^{2+}_{y}Mn^{3+}_{1.4-2y}Mn^{4+}_{0\cdot6+y}]\ O^{2-}_{4};$$
with $0{\cdot}6 < x \leq 1$ and $y = x - 0{\cdot}6$.

This first structural approach of the solid solution gives a good base for the next step that will be the fine characterization of these components by neutron diffraction and magnetic measurements. With only one solid solution, the electrical resistivities of these thermistors cover a wide range: $>2\ 10^6\ \Omega$ cm – 10 Ω cm and might be interesting for industrial applications.

Acknowledgements

The authors would like to thank H. Minchin for the preparation of several samples and the French scholarship program, 'Lavoisier', without which this paper would not have been written.

References

1. Kulkarni, D. K. & Mande, C., X-ray spectroscopic study of some copper manganites. *Indian Journal of Pure and Applied Physics*, **12** (1974) 60–3.
2. Brabers, V. A. M. & Setten, F., X-ray photoelectron spectroscopy study of ionic configuration of the spinel $CuMnCoO_4$. *J. Phys. D: Appl. Phys.*, **16** (1983) 160–71
3. Kshirsagar, S. T. & Biswas, A. R., Crystallographic studies of some mixed manganite spinels. *J. Phys. Chem. Solids*, **28** (1967) 1493–9.
4. Jabry, E., Elaboration et caractérisation de céramiques semi-conductrices destinées aux thermistances C.T.N., PhD, Toulouse, France (1987).
5. Irani, K., Sinha, A. & Biswas, A., Effect of temperature on the structure of manganites., *J. Phys. Chem. Solids*, **23** (1962) 711–27.
6. Driessens, F. C. M., Place and valence of the cations in Mn_3O_4 and some related manganates. *Inorg. Chemica. Acta*, **I**:1 (1967) 193–201.
7. Wickam, D. G. & Croft, W. J., Crystallographic and magnetic properties of several spinels containing trivalent manganese. *J. Phys. Chem. Solids*, **7** (1958) 351–60.
8. Metz, R., Elaboration et caractérisation de céramiques semi-conductrices à base de manganites de nickel, cobalt et cuivre. Etude des phénomènes de vieillissement des thermistances à coefficient de température négatif. (C.T.N.), PhD, Toulouse University, France, (1991).
9. Metz, R., Caffin, J. P., Legros, R. & Rousset, A., The preparation, characterization and electrical properties of copper manganite spinels $Cu_xMn_{3-x}O_4$, $0 \leq x \leq 1$. *J. Mater. Sci.*, **24** (1989) 83–7.
10. Baffier, N. & Huber, M., Etude par diffraction des rayons X et des neutrons des relations entre distribution cationique et distorsion cristalline dans les ferro–manganites spinelles $x Mn_3O_4$ + (1-x) $Cu(Fe,Cr)O_4$, *Ibid.* **33** (1972) 737–47.
11. Poix, P., Sur une méthode de détermination des distances cation-oxygène dans les oxydes mixtes à structure spinelle, application des valeurs à quelques cas particuliers. *Bull Soc. Chim., France*, **5** (1965) 1085–7.
12. Dorris, S. E. & Masson, T. O., Electrical properties and cation valencies in Mn_3O_4. *J. Ann. Ceram. Soc.*, **71** (1988) 379–85.